Neuron, Vol. 41, 257–268, January 22, 2004, Copyright ©2004 by Cell Press

Bidirectional Modification of Presynaptic Neuronal Excitability Accompanying Spike Timing-Dependent Synaptic Plasticity

Cheng-yu Li,[1,3] Jiang-teng Lu,[1,3] Chien-ping Wu,[1] Shu-min Duan,[1,*] and Mu-ming Poo[1,2,*]
[1]Institute of Neuroscience
Chinese Academy of Sciences
Shanghai Institute of Biological Sciences
Shanghai 200031
China
[2]Division of Neurobiology
Department of Molecular and Cell Biology
University of California
Berkeley, California 94720

Summary

Correlated pre- and postsynaptic activity that induces long-term potentiation is known to induce a persistent enhancement of the intrinsic excitability of the presynaptic neuron. Here we report that, associated with the induction of long-term depression in hippocampal cultures and in somatosensory cortical slices, there is also a persistent reduction in the excitability of the presynaptic neuron. This reduction requires postsynaptic Ca^{2+} elevation and presynaptic PKA- and PKC-dependent modification of slow-inactivating K^+ channels. The bidirectional changes in neuronal excitability and synaptic efficacy exhibit identical requirements for the temporal order of pre- and postsynaptic activation but reflect two distinct aspects of activity-induced modification of neural circuits.

Introduction

Persistent changes in neural circuits induced by electrical activity are essential for experience-dependent refinement of the developing nervous system (Katz and Shatz, 1996; Zhang and Poo, 2001) and for learning and memory functions of the mature brain (Hebb, 1949; Bliss and Collingridge, 1993; Martin et al., 2000). In many parts of the central nervous system, a brief period of electrical activity can induce long-term potentiation (LTP) or long-term depression (LTD) of synaptic transmission (Bliss and Lømo, 1973; Malenka and Nicoll, 1999; Bear and Linden, 2001). In addition to these changes in synaptic efficacy, there is now increasing evidence that the intrinsic excitability of pre- and postsynaptic neurons is also regulated by electrical activity. Alteration of neuronal excitability may be induced by chronic modulation of neuronal firing (Turrigiano et al., 1994; Marder et al., 1996; Desai et al., 1999; Nick and Ribera, 2000) or by a brief period of tetanic activity (Aizenman and Linden, 2000; Armano et al., 2000; Ganguly et al., 2000). In the hippocampus, increased probability of neuronal spiking occurs in parallel with the tetanus-induced LTP (Bliss and Lømo, 1973; Taube and Schwartzkroin, 1988; McNaughton et al., 1994; Daoudal et al., 2002). Part of this apparent increase in excitability can be accounted for by postsynaptic changes of active conductances in the dendrite (Wathey et al., 1992). Neuronal excitability can also be increased in rabbit hippocampal CA1 region after trace eye blink conditioning (Moyer et al., 1996). On the presynaptic side, activity-induced long-term facilitation at crayfish neuromuscular junctions (Beaumont et al., 2002) and LTP of mossy fiber-CA3 synapses in the hippocampus (Mellor et al., 2002) have both been reported to result from modifications of presynaptic I_h channels. In cultures of hippocampal neurons, induction of LTP by correlated pre- and postsynaptic activation is accompanied by an immediate and persistent enhancement of the intrinsic neuronal excitability of the presynaptic neuron, a modification that was caused by enhanced gating properties of Na^+ channels (Ganguly et al., 2000).

In the present study, we examined whether there is also alteration of intrinsic neuronal excitability following the induction of LTD by correlated pre- and postsynaptic activation. Using simultaneous whole-cell recording in pre- and postsynaptic neurons in hippocampal cultures and in somatosensory cortical slices, we showed that LTD induction at synapses between glutamatergic neurons is accompanied by a reduction of the global intrinsic excitability of the presynaptic neuron. In cultured neurons, this presynaptic change can be attributed to an enhanced activation of voltage-dependent slow-inactivating K^+ channels. Furthermore, we found that this presynaptic modification requires postsynaptic Ca^{2+} elevation and presynaptic activation of both PKA and PKC. Together with the previous finding on LTP-related enhancement of presynaptic excitability (Ganguly et al., 2000), these results demonstrate that correlated pre- and postsynaptic activation can induce bidirectional modification of presynaptic excitability. Such presynaptic changes require an immediate retrograde signaling across the synapse and a rapid spread of cytosolic signals throughout the presynaptic neuron, leading to global modification of ion channels.

Results

Bidirectional Modulation of Presynaptic Firing Properties

Cultured rat hippocampal neurons were prepared from E17 to E20 rat embryos and used after 8 to 20 days in vitro (Bi and Poo, 1998). Dual perforated whole-cell recordings were made from pairs of neurons that formed functional synapses. The nature of the synaptic connection (glutamatergic versus GABAergic) was determined by the time course, the reversal potential and, in some cases, the sensitivity of the synaptic currents to specific pharmacological blockers (see Experimental Procedures). To assay presynaptic neuronal excitability, trains of action potentials were evoked in the presynaptic neuron (current clamped at −70 mV) by injecting prolonged depolarizing currents (0.03–0.2 nA, 300 ms) at a low

*Correspondence: shumin@ion.ac.cn (S.-m.D.), mpoo@uclink.berkeley.edu (M.-m.P.)
[3]These authors contributed equally to this work.

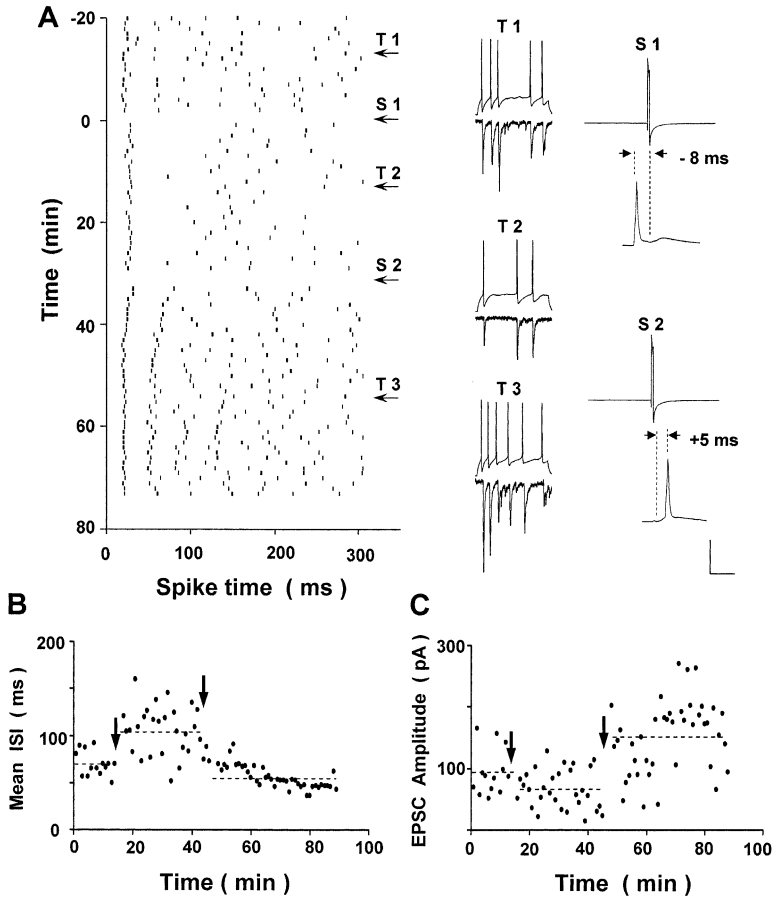

Figure 1. Changes in Firing Property of Presynaptic Neuron Induced by Repetitive Correlated Synaptic Activity in Cultured Hippocampal Neurons

(A) Representative raster plot of spike times during injection of a step-depolarizing current (300 ms) into the presynaptic neuron. Repetitive correlated pre- and postsynaptic stimuli (1 Hz for 80 s) were applied at time 0 and 30 min to induce LTD and LTP, respectively, using a negative (−8 ms, post before pre, S1) and a positive (+5 ms, pre before post, S2) interval. Sample test traces on the right (T1, T2, and T3) depict paired recordings of the firing pattern of the presynaptic neuron under current clamp (c.c., $V_c = -70$ mV) in response to a standard step depolarization and of EPSCs in the postsynaptic neuron under voltage clamp (v.c., $V_c = -70$ mV) at the times marked by the arrows. Spike time 0 refers to the onset of 300 ms depolarizing step. Scales for T1–T3: 50 mV (pre) or 50 pA (post), 100 ms. Also shown are sample paired recordings of membrane potentials of pre- and postsynaptic neurons (S1 and S2) during repetitive co-activation at 0 and 30 min marked by the arrows. Scales for S1 and S2: 1.0 nA (pre) or 50 mV (post), 10 ms.

(B) The mean interspike interval (ISI) of the presynaptic spiking induced by the step depolarization before and after correlated activation (marked by arrows) that induced LTD and LTP, respectively, for the experiment described in (A). Dotted lines depict average values during the three periods.

(C) The peak amplitude of the first EPSCs ($V_c = -70$ mV) evoked by the presynaptic step-depolarization test stimuli at various times before and after the correlated stimulation, for the experiment described in (A).

frequency (0.017 Hz). The mean interspike interval (ISI) of action potentials was used as a parameter for the firing characteristics. The synaptic strength between the pair of recorded neurons was monitored by the amplitude of the first excitatory postsynaptic current (EPSC) evoked by a train of action potentials.

In the first set of experiments, we examined the effect of correlated pre- and postsynaptic activity that is known to induce LTP or LTD at glutamatergic synapses in these hippocampal cultures (Bi and Poo, 1998). Repetitive step-depolarizations (1 ms, +150 mV) were applied to the presynaptic neuron ($V_c = -70$ mV, 1 Hz, 80 s), each paired with a postsynaptic action potential, either before ("negative" intervals) or after ("positive" intervals) the presynaptic stimulation. An example of the recording from a pair of glutamatergic neurons is shown in Figure 1. Following repetitive coactivation of the neurons at a negative interval of −8 ms (post/pre, S1 in Figure 1A), there was a persistent reduction in the amplitude of the first EPSC. Subsequent repetitive coactivation of the same pair of neurons at an interval of +5 ms (pre/post, S2 in Figure 1A) resulted in a persistent elevation of the amplitude of the first EPSC. Accompanying the sequential induction of LTD and LTP, we observed an increase and a decrease in the mean ISI in the presynaptic neuron, respectively, as assayed by repetitive injections of an identical step-depolarizing current (Figures 1B and 1C). Thus, there were bidirectional modifications of both synaptic efficacy and presynaptic firing properties.

Similar recordings were made from many connected pairs of hippocampal neurons, using correlated activation at different time intervals. For 16 neuronal pairs in which LTD was induced by coactivation at negative intervals in the range of −15 to −5 ms, there was a consistent increase in the mean ISI of the presynaptic neuron following LTD induction (Figures 2A and 2B). At 10–20 min after coactivation of the neuronal pairs with reciprocal connections ($n = 11$), the mean ISI increased by 35% ± 16% (mean ± SEM) and the EPSC amplitude decreased by 38.6% ± 9.6% (mean ± SEM). Similar changes were observed in neuronal pairs with ($n = 11$) or without ($n = 5$) recurrent connections, suggesting that the observed changes in presynaptic firing were unlikely to result from the presence of recurrent connections. Ganguly et al. (2000) had previously reported a decreased threshold for spiking after LTP induction. Here we observed an increased threshold for spiking after LTD (from −43.8 ± 4.1 to −37.5 ± 5.7 mV, SEM, $n = 4$, $p < 0.05$, paired t test). In agreement with Ganguly et al. (2000), we also observed a persistent reduction in the mean ISI (Figures 2C and 2D) following the induction of LTP by repetitive coactivation at positive intervals (+3 to +10 ms). At 10–20 min after correlated activation, the mean ISI decreased by 34.1% ± 6.1% (SEM, $n = 6$)

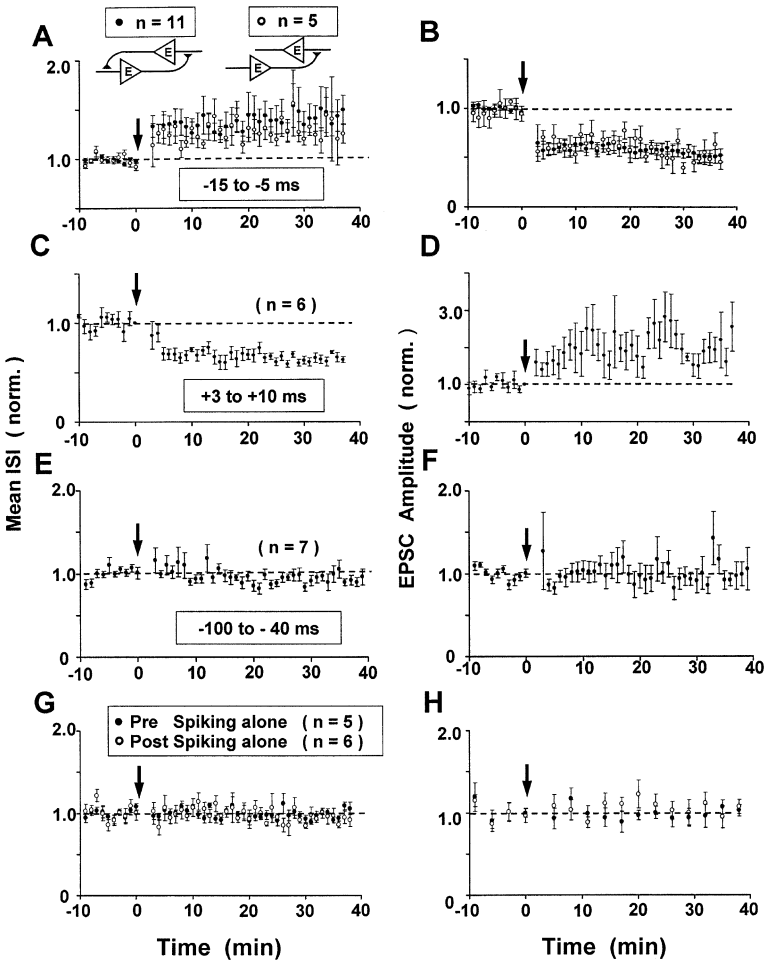

Figure 2. Changes in the Presynaptic Firing Property Induced by Repetitive Correlated Activation at Different Intervals in Cultured Hippocampal Neurons

(A and B) Elevation of the mean ISI accompanying the induction of LTD by correlated activation at negative intervals (−15 to −5 ms). Results for glutamatergic neuronal pairs are separated into two groups (see diagram above): those reciprocally connected (n = 11, filled circles) and those containing no recurrent connections (n = 5, open circles). Data points (mean ± SEM, n = total number of experiments) were normalized by the average value during the control period prior to repetitive coactivation. Dotted lines depict average values during the control periods.

(C and D) Reduction of the mean ISI accompanying the induction of LTP by correlated activation at positive intervals (+3 to +10 ms).

(E and F) No change in the mean ISI and synaptic strength by correlated activation at large negative intervals (−100 to −40 ms).

(G and H) No change in the mean ISI and synaptic strength following repetitive stimulation of the pre- (n = 5, filled circles) or postsynaptic (n = 6, open circles) neuron alone, with the post- or presynaptic neuron voltage-clamped at −70 mV, respectively.

and the EPSC amplitude increased by 79% ± 26% (SEM, n = 6). Consistent with the bidirectional modulation of ISI, there were corresponding changes in the total spike number during a 300 ms step depolarization. The spike number decreased by 25.0% ± 3.3% (SEM, n = 16; $p < 0.001$) after LTD induction and increased by 37.6% ± 9.1% (SEM, n = 6; $p < 0.005$) after LTP induction. In contrast to the above results, repetitive coactivation at spike timing intervals in the range of −100 to −40 ms failed to induce any modification of either synaptic strength or presynaptic excitability (Figures 2E and 2F). Furthermore, pre- or postsynaptic activation alone (at 1 Hz for 80 s) was also ineffective (Figures 2G and 2H). Similarly, repetitive postsynaptic activation alone had no effect on mean ISIs observed in the postsynaptic neurons (see Supplemental Figure S1 at http://www.neuron.org/cgi/content/full/41/2/257/DC1). Thus, changes in the presynaptic firing properties were due to a specific temporal relationship between pre- and postsynaptic activation.

Throughout these experiments, the presynaptic membrane potential remained unchanged. It was −70.7 ± 1.7 mV at 0–10 min before and −70.1 ± 1.5 mV (SEM, n = 16, p = 0.93, paired t test) at 10–20 min after correlated activation at negative intervals. For positive intervals, it was −70.6 ± 0.79 mV and −69.5 ± 0.71 mV (SEM, n = 6, p = 0.20), respectively. In addition, when marked changes in the mean ISI were observed, the input resistance of the presynaptic neuron remained stable (97% ± 2.7% of the control value at 10–20 min after correlated activity of negative intervals, n = 16, p = 0.81; 96% ± 5.3%, n = 6, p = 0.66 for positive intervals). Thus, the observed alteration in the presynaptic firing was unlikely to result from activity-induced changes in passive membrane properties, at least at the soma. Furthermore, the constancy in the membrane potential changes induced by injection of step hyperpolarizing current during measurement of input resistance suggests that I_h channels are not involved in the changes in presynaptic excitability (see below).

Dependence on the Spike Timing

Previous studies in several systems have shown that the induction of LTP/LTD depends critically on the relative timing of the pre- and postsynaptic spikes (Markram et al., 1997; Debanne et al., 1998; Zhang et al., 1998; Bi and Poo, 1998; Feldman, 2000; Nishiyama et al., 2000; Froemke and Dan, 2002). We have systematically examined the presynaptic firing property following correlated pre- and postsynaptic activation at different spike timing intervals from −100 to +100 ms. As shown in Figure 3, we observed a marked correspondence between the time windows for activity-induced changes in the mean ISI and synaptic efficacy, both requiring that the interval

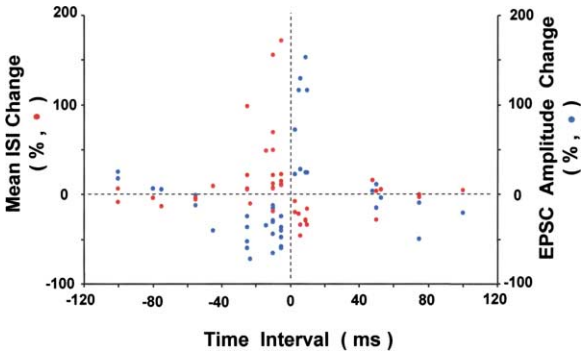

Figure 3. Dependence on the Timing of Pre- and Postsynaptic Activation

Summary of changes in the mean ISI of presynaptic firing and in the amplitude of the first EPSC following correlated pre- and postsynaptic activation at different intervals. Each data point represents result from one experiment. The percentage changes for ISI (red) and EPSC amplitude (blue) were calculated from the mean value at 10–20 min after correlated activation, as compared to the mean value during the control period. The interval refers to the time between the onset of the EPSP and the peak of the postsynaptic spike.

between the pre- and postsynaptic activation lie within about ±20 ms. Increase and decrease in the presynaptic firing frequency tightly correlate with synaptic potentiation and depression, respectively.

Reduction of Presynaptic Excitability Associated with LTD in Cortical Slices

In order to determine whether the above finding obtained in cell cultures also occurs in a more intact neural tissue, we have examined the modulation of presynaptic excitability after LTD induction in somatosensory cortical slices obtained from P12–P16 rats (see Experimental Procedures). Excitatory neurons were selected based on morphological criteria and the pattern of spiking during injection of a depolarizing current (Figures 4A and 4B; McCormick et al., 1985; Feldmeyer et al., 1999). Dual whole-cell patch recording from two synaptically connected excitatory neurons in layers 2/3 and 4 was made (Feldmeyer et al., 1999; Egger et al., 1999), and LTD was induced using correlated pre- and postsynaptic activation at negative intervals. Perforated patch recording was used for the presynaptic cell in order to obtain reliable measurement of presynaptic ISI (see Experimental Procedures). Repetitive depolarizations (1.0 to 1.6 ms, +100 mV) were applied to the pre- and postsynaptic neurons (in current clamp, 0.5–1 Hz for 3 to 6 min), with a negative time interval of −10 to −5 ms (post/pre, see Figure 4B). In 21 cases examined, the amplitude of the first EPSPs decreased by 19.7% ± 5.9% (SEM, $p < 0.01$, paired t test; Figure 4D) at 20 to 30 min after the coactivation and the presynaptic ISI increased by 17.6% ± 6.5% (SEM, $p < 0.01$). In contrast, repetitive correlated activation of similar pattern but the interval of −200 to −100 ms ($n = 9$) failed to induce any significant change in either ISI or EPSP amplitude (Figure 4E). In these experiments, changes in the input resistance were less than 10% and showed no correlation with the extent of changes in either ISI or EPSP. These results from acute cortical slices are fully consistent with the findings in hippocampal cultures described above.

Dependence on the Postsynaptic Cell Type

In addition to the synapses between pairs of glutamatergic neurons, we have also examined glutamatergic synapses onto GABAergic neurons (E→I) in hippocampal cultures. As shown in Figures 5A and 5B, repetitive coactivation at intervals of −8 to −6 ms, which normally induces an increase in presynaptic ISI and LTD of E→E synapses, was ineffective in modifying either synaptic efficacy or the presynaptic firing property. This result is consistent with previous findings that at these E→I synapses correlated pre- and postsynaptic activation failed to induce LTP (Bi and Poo, 1998) or to enhance the excitability of the presynaptic neuron (Ganguly et al., 2000). Thus, there appears to be a tight link between synaptic plasticity and changes in the presynaptic firing property, suggesting common underlying mechanisms.

Changes in the Intrinsic Excitability

The decreased presynaptic firing frequency in response to depolarization accompanying the induction of LTD may result from a reduction in the intrinsic excitability of the presynaptic neuron or a stimulation-induced reduction of the background synaptic drive received by the presynaptic neuron, e.g., a reduced tonic glutamatergic input or an increased GABAergic inhibition (Lu et al., 2000). To test this possibility, we examined the firing property of the presynaptic neuron after glutamatergic and GABAergic transmission was abolished by perfusing the culture with specific antagonists of non-NMDA, NMDA, and $GABA_A$ receptors, i.e., DNQX, D-APV, and bicuculline, respectively. During the period of correlated activation, however, these blockers were washed out and replaced with normal recording solution to allow synaptic activation. As shown in Figures 5C and 5D, we observed a consistent increase in the mean ISI (36.9% ± 6.9% of the control, SEM, $n = 5$) in the absence of synaptic transmission following correlated activation (at an interval of −8 ms) that induced LTD. These results indicate that a reduction of intrinsic excitability is likely to be the cause of reduced presynaptic firing in response to depolarization.

Requirement of Postsynaptic Ca^{2+} Elevation

Calcium influx into the postsynaptic neuron following correlated pre- and postsynaptic activation is critical for the induction of LTP and LTD, which require activation of NMDA receptors and/or L-type Ca^{2+} channels at some synapses (Koester and Sakmann, 1998; Bi and Poo, 1998; Malenka and Nicoll, 1999). In the present study, we have examined whether NMDA receptors and L-type Ca^{2+} channels are also involved in the modification of presynaptic excitability. Nifedipine (10 μM), a specific L-type Ca^{2+} channel blocker, was added to the bath 3 min before correlated activation (at an interval of −8 and +5 ms). As shown in Figures 6A to 6B, this treatment abolished both LTD and the reduction of presynaptic excitability, but did not block LTP and the increase of presynaptic excitability (Figures 6C and 6D), consistent with the previous finding (Bi and Poo, 1998). Surprisingly, bath application of D-APV (50 μM), although it

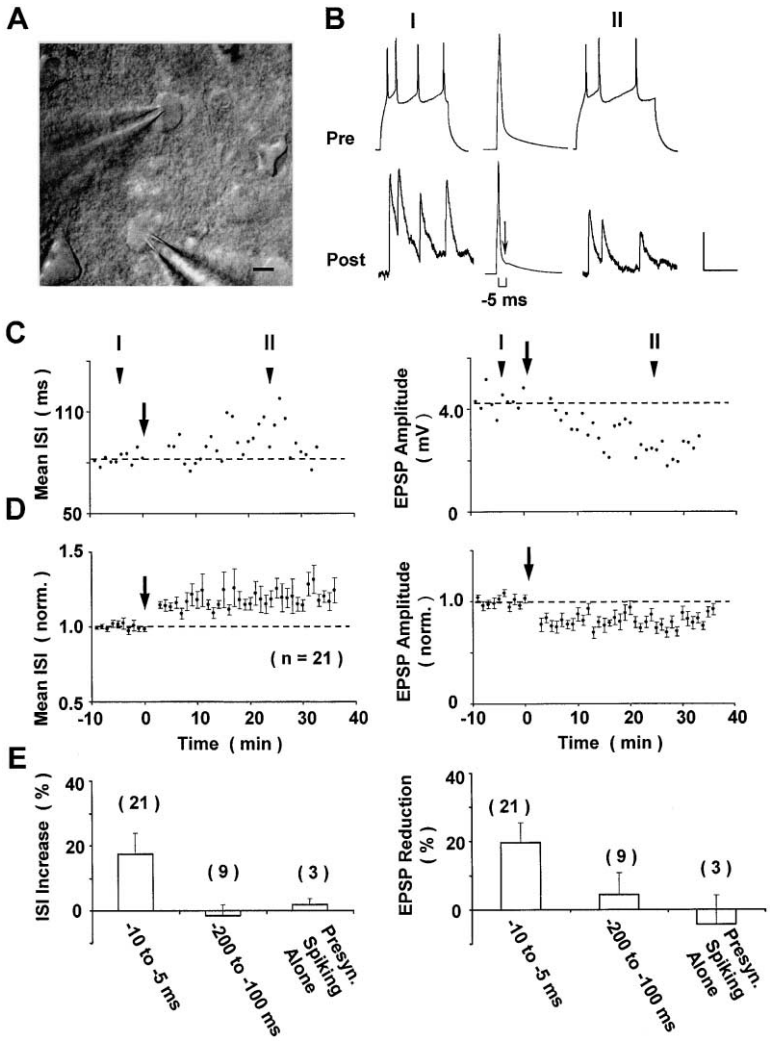

Figure 4. Reduction of Presynaptic Excitability Accompanying LTD in Somatosensory Cortical Slices

(A) DIC image of two connected layer 4 spiny neurons, with recorded responses shown in (B) and (C). Scale bar equals 10 μm.

(B) Typical presynaptic bursting spiking caused by injection of a step current (240 pA, 300 ms) and postsynaptic responses before (I) and after (II) repetitive correlated activation (0.5 Hz for 360 s at an interval −5 ms, middle traces, in c.c.). Arrow indicates the onset of EPSP elicited by the presynaptic spike. Scale bars for I and II equal 50 (pre) or 2.0 (post) mV, 100 ms. Scale bars for correlated activation equal 50 mV, 20 ms.

(C) Left: The mean ISI of presynaptic firing elicited by a step-depolarization test stimuli. Right: The peak amplitude of the first EPSPs (V_c = −70 mV) before and after correlated activation (arrow), for the experiment described in (B).

(D) Summary of the change in the mean ISI accompanying the induction of LTD by correlated activation at negative intervals (−10 to −5 ms).

(E) Summary of ISI changes and synaptic modification for all slice experiments, using repetitive correlated spiking at intervals of −10 to −5 ms or −200 to −100 ms, and presynaptic spiking alone (at the same frequency). The histograms represent mean percentage change in ISI (left) and reduction in EPSP amplitude (right) at 20–30 min after correlated spiking. The number in the parentheses depicts the number of neuron pairs recorded. Only data for −10 to −5 ms interval were significantly different from the control value before correlated spiking.

blocked LTP induction and ISI change (data not shown), had no significant effect on the induction of LTD (−43.2% ± 2.0%, n = 6, Figure 6F) and the reduction of presynaptic excitability (ISI increased by 58.0% ± 3.8%, n = 6, Figure 6E) induced by the correlated activity. This lack of APV effect does not agree with that previously reported (Bi and Poo, 1998). The discrepancy may result from the use of different culture media, which consist of serum supplements from different sources (see Experimental Procedure). Distinct trophic factors in the serum may result in differences in the expression of NMDA receptors, Ca^{2+} channels, Ca^{2+} buffering proteins, or other cytoplasmic signaling mechanisms, leading to differences in the relative contributions of various Ca^{2+} sources involved in activity-induced Ca^{2+} elevation. To further examine the role of postsynaptic Ca^{2+} signaling, we loaded a rapid Ca^{2+} buffer BAPTA-AM (2 mM) into the postsynaptic neuron via the perforated-patch recording pipette. The effectiveness of BAPTA loading was confirmed by the appearance of coloaded membrane-permeable fluorescence markers along the nerve processes (data not shown) and the concurrent reduction in synaptic output of the loaded neuron (Ganguly et al., 2000). When correlated activation of pre- and postsynaptic neurons (1 Hz, 80 s, interval −8 ms) was applied 40 min following the onset of loading, we found no significant change in either synaptic efficacy or presynaptic excitability (Figures 6G and 6H). Calcium release from intracellular stores is known to be crucial for the induction of LTD (Nishiyama et al., 2000). Consistent with this, we found that treatment with thapsigargin (1.0 μM) prior to and during the experiment abolished both LTD and reduction of presynaptic excitability (Figures 6G and 6H). Thus, postsynaptic Ca^{2+} elevation resulting from Ca^{2+} influx through L-type Ca^{2+} channels and Ca^{2+} release from intracellular stores are required for the induction of LTD and the reduction in presynaptic neuronal excitability.

The Role of Presynaptic PKC and PKA

Changes in intrinsic neuronal excitability are likely to result from modulation of active conductances, e.g., through phosphorylation of various voltage-dependent ion channels by protein kinase C (PKC) and protein kinase A (PKA) (Madison and Nicoll, 1986; Hu et al., 1987; West et al., 1991; Schroeder et al., 1998; Hoffman and Johnston, 1998; Beaumont et al., 2002). Ganguly et al. (2000) reported that presynaptic PKC, but not PKA activ-

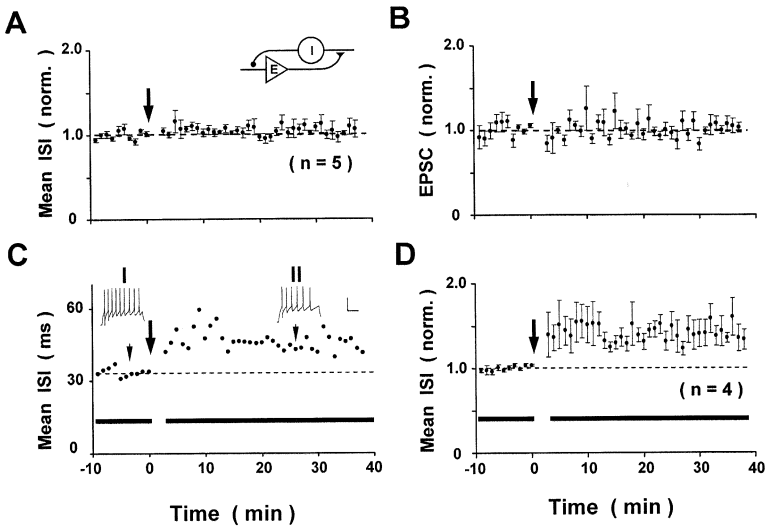

Figure 5. Changes in the Firing Property Are Dependent on Postsynaptic Cell Type and Independent of Synaptic Drive

(A and B) No change in the mean ISI and synaptic strength following repetitive correlated activation (at intervals of −8 to −6 ms) of glutamatergic synapses when the postsynaptic neuron was GABAergic (I). All five pairs recorded were reciprocally connected (see diagram above).

(C) The change in the presynaptic firing property induced by correlated activation is not due to increased synaptic drive. Data from a representative experiment are shown. The ISI of presynaptic spiking triggered by a step depolarization (300 ms) was measured in the presence of D-APV (50 μM), DNQX (2.0 μm), and bicuculline (10 μm), as marked by the bar, except for the 2 min period of repetitive coactivation, during which the drugs were washed out by perfusing the culture with fresh recording solution.

(D) Summary of all experiments similar to that shown in (C). The mean ISI measured in each experiment was normalized to the mean value during the control period.

ity, is required for the enhancement of presynaptic neuronal excitability following the correlated activation that induces LTP. In the present study, we examined whether blocking PKC or PKA activity in the presynaptic neuron affects LTD induction and the reduction of presynaptic excitability. As shown in Figures 7A and 7B, induction

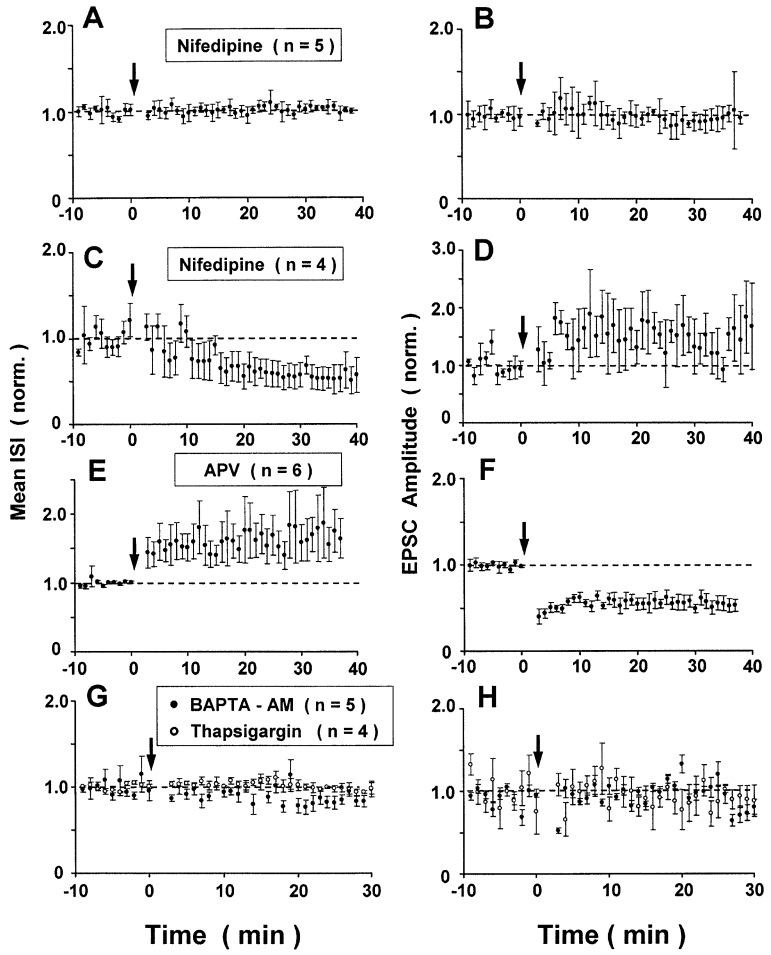

Figure 6. Dependence on the Postsynaptic Ca^{2+} Elevation

(A and B) No change in the mean ISI and synaptic strength following repetitive correlated activation at a negative interval (−8 ms) in the presence of nifedipine (10 μM).

(C and D) Reduction in the mean ISI and enhancement of synaptic response following repetitive activation at a positive interval (+5 ms) in the presence of nifedipine (10 μM).

(E and F) Elevation of the mean ISI accompanying the induction of LTD by correlated activation at negative intervals (−10 to −8 ms) in the presence of D-APV (50 μM).

(G and H) No change in the mean ISI and synaptic strength following correlated activation at negative intervals (−10 to −8 ms), in the presence of pipette-loaded BAPTA-AM (2 mM) in postsynaptic cells or bath-applied thapsigargin (1.0 μM).

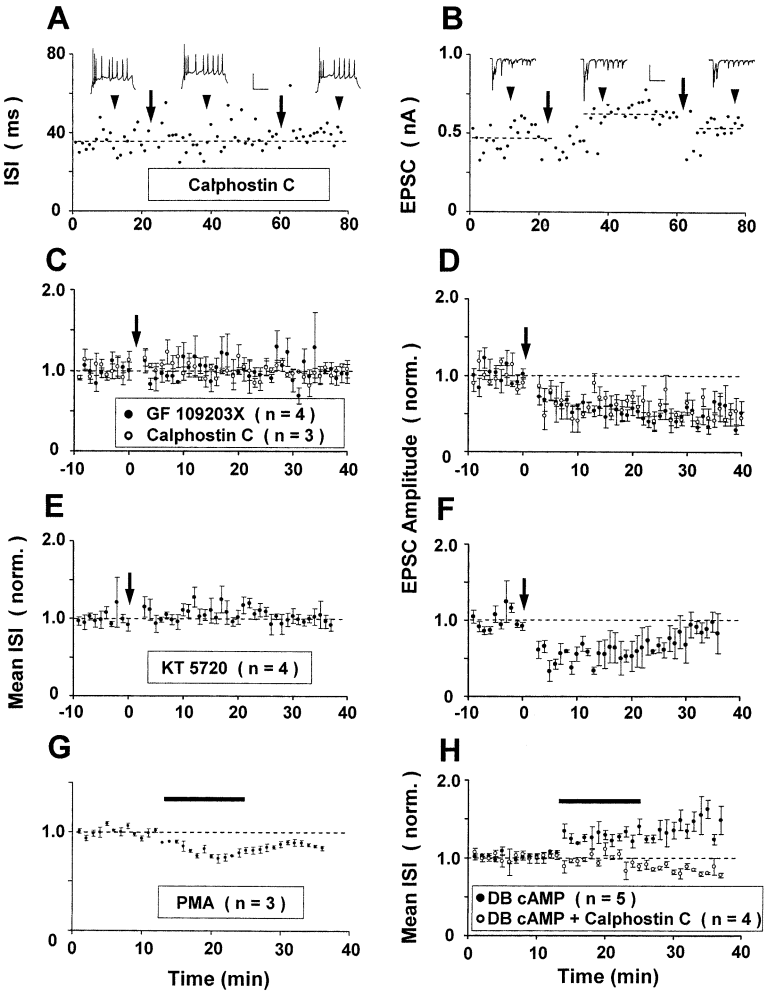

Figure 7. Dependence on Presynaptic PKC and PKA Activities

(A and B) An example experiment in which the presynaptic neuron was loaded with the PKC inhibitor Calphostin C (100 nM) through the perforated patch pipette. No change in the mean ISI of presynaptic firing was found following the induction of LTP (A) and LTD (B) by correlated activation at positive (+6 ms) and negative (−8 ms) intervals, respectively, at the times marked by arrows. Sample traces above depict presynaptic firing patterns (A) and postsynaptic EPSCs (B) at the time marked by the arrowhead. Scale bars equal 50mV (200 pA), 100 ms.

(C and D) Presynaptic loading of the PKC inhibitor, GF 109203X (50 nM) or Calphostin C (100 nM), abolished changes in the mean ISI induced by correlated activation, without affecting the induction of LTD.

(E and F) Presynaptic loading of a PKA inhibitor KT 5720 (1.0 μM) abolished the changes in the mean ISI induced by correlated activation, without affecting the induction of LTD.

(G and H) Effects of PKC activation and PKA/PKC co-activation. In (G), bath application of PMA (1.0 nM, duration marked by the bar) reduced the mean ISI. In (H), bath application of dB-cAMP (100 μM) increased the mean ISI, but the effect was abolished by the co-application of Calphostin C (100 nM).

of LTP and LTD by correlated activity was not affected when the presynaptic neuron was loaded with specific PKC inhibitor Calphostin C (100 nM) through the perforated patch pipette, but the mean ISI remained unchanged throughout the experiment. The results of all experiments using the LTD-inducing protocol and presynaptic loading of specific PKC inhibitors GF 109203X (Bisindolylmaleimide I Hydrochloride, 50 nM) or Calphostin C (100 nM) are summarized in Figures 7C and 7D. Similarly, presynaptic loading with a specific PKA inhibitor KT 5720 (1.0 μM) also blocked the change in the mean ISI without significantly disrupting LTD induction (Figures 7E and 7F). Thus, both PKC and PKA activities in the presynaptic neuron are necessary for the reduction of presynaptic excitability following correlated activation that induces LTD.

Previous studies have shown that activation of PKC or PKA can modulate somatic (Madison and Nicoll, 1986) or dendritic (Hoffman and Johnston, 1998) excitability. We have also examined in the present culture system whether direct activation of PKC or PKA is sufficient to induce bidirectional modification of presynaptic excitability. As shown in Figure 7G, bath application of a low concentration of PKC activator PMA (phorbol 1,2-myristate 1,3-acetate, 1.0 nM) can significantly enhance the neuronal firing, with a 21.5% ± 6.8% (n = 3) reduction in the mean ISI at 5–15 min after the drug treatment. In contrast, application of dibutyryl cAMP (dB-cAMP, 100 μM), a membrane-permeable analog of cAMP, significantly decreased the neuronal firing, with 34.8% ± 9.0% (n = 5) increase in the mean ISI (Figure 7H). Because presynaptic loading of PKC inhibitors was found to prevent the ISI increase induced by the LTD protocol (Figure 7C), we further tested whether PKC activity is necessary for the action of PKA in reducing neuronal firing. As shown in Figure 7H, co-application of Calphostin C (100 nM) together with dB-cAMP (100 μM) indeed abolished the effect of dB-cAMP on neuronal excitability. Taken together, these results suggest that a basal PKC activity in the neuron is necessary for PKA-dependent processes to reduce neuronal excitability.

Enhancement of K^+ Channel Activation

To further understand the mechanism underlying the observed reduction of presynaptic excitability, we examined whether there is any change in K^+ channel activation kinetics following repetitive correlated activation. We first examined the slow-inactivating K^+ channels by blocking the Na^+ channels with tetrodotoxin (1 μM), Ca^{2+} channels and Ca^{2+}-dependent K^+ channels with Cd^{2+} (100 μM), and A type K^+ channels with 4-AP (2 mM) (see Supplemental Figure S2 at http://www.neuron.org/

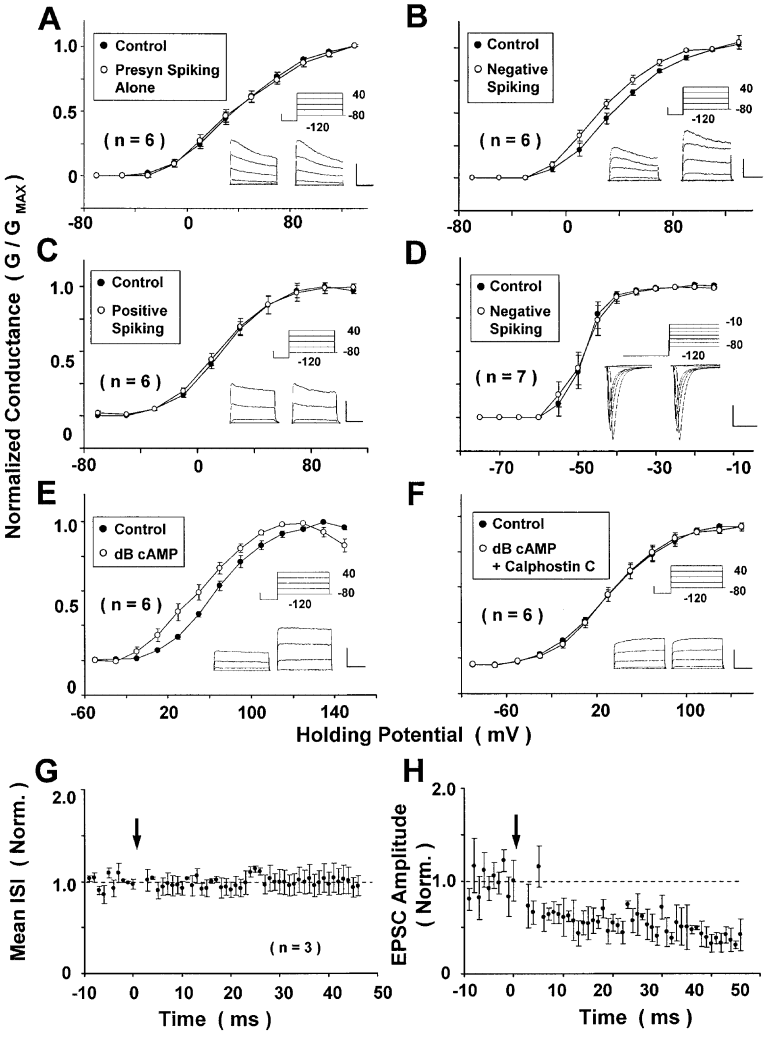

Figure 8. Changes in the Activation Kinetics of Slow-Inactivating K^+ Channels of the Presynaptic Neuron Following Correlated Activity

(A) Effects of repetitive presynaptic activation. Data recorded in the presence of TTX (1.0 μM), $CdCl_2$ (100 μM), 4-AP (2.0 mM), and DNQX (2.0 μM). Voltage-dependent activation of K^+ currents (averaged amplitude of the plateau current at 200 to 300 ms during the depolarization) before (filled circles) and after (open circles) repetitive presynaptic activation, with postsynaptic neuron held at $V_c = -70$ mV. Data points represent K conductance (G) observed at various test pulse potentials normalized to the maximal value (G_{max}). $V_{1/2} = 27.3 \pm 1.8$ mV (SEM, slope 27.0) during the control period and $V_{1/2} = 25.9 \pm 2.4$ mV (slope 29.3) at 5 min after the presynaptic spiking ($p > 0.3$, paired t test). Also shown are sample traces of K^+ currents recorded at various step potentials (−80 to +40 mV, Δ20 mV) before (left) and after (right) presynaptic activation. Scale bars equal 100 ms, 2.0 nA.

(B) Effects of correlated activation at a negative interval (−6 ms) on K^+ currents. Experiments similar to those in (A), except that correlated pre- and postsynaptic activation was applied. $V_{1/2} = 25.5 \pm 1.6$ mV (slope 22.4) during the control period and $V_{1/2} = 15.4 \pm 1.9$ mV (slope 21.1) at 5 min after correlated activation. The difference is significant ($p < 0.01$, paired t test).

(C) Effects of correlated activation at positive intervals. Experiments similar to those in (B), except that the positive interval of +5 ms was used. $V_{1/2} = 24.1 \pm 2.6$ mV (slope 13.6) during the control period and $V_{1/2} = 25.0 \pm 1.6$ mV (slope 15.7) at 5 min after the correlated activation ($p > 0.5$, paired t test).

(D) Effects of correlated activation at negative intervals (−6 ms) on activation of Na^+ currents, recorded at various step potentials (−80 to −10 mV, Δ5 mV). Experiments similar to those in (B), but replacing K-gluconate in the pipette solution with CsCl (55 mM) and $CsCH_3O_3$ (75 mM) and perfusing the bath with $CdCl_2$ (100 μM), CsCl (50 mM), 4-AP (5 mM), TEA-Cl (30 mM), D-APV (25 μM), DNQX (2.0 μM), and Picrotoxin (100 μM). $V_{1/2} = -41.3 \pm 0.9$ mV (slope 3.0) during the control period and $V_{1/2} = -41.5 \pm 1.9$ mV (slope 2.1) at 5 min after correlated activation ($p > 0.5$, paired t test). Scale bars equal 5 ms, 2.0 nA.

(E) Effects of PKA activation on K^+ currents. Experiments similar to those in (B), except that correlated activation was replaced by bath application of dB-cAMP (100 μM). $V_{1/2} = 35.6 \pm 1.0$ mV (slope, 24.4) during the control period and $V_{1/2} = 14.3 \pm 4.2$ mV (slope, 24.3) at 5 min after the drug application. The difference is significant ($p < 0.01$, paired t test).

(F) Effects of co-activation of PKA and PKC on K^+ currents. Experiments similar to those in (C), except that Calphostin C (100 nM) was bath-applied together with dB-cAMP (100 μM). $V_{1/2} = 40.5 \pm 0.7$ mV during the control period and $V_{1/2} = 39.9 \pm 0.8$ mV at 5 min after application of the drugs ($p > 0.3$, paired t test).

(G and H) Effects of TEA (10 mM) on the excitability change and synaptic modification induced by correlated activation at a negative interval (−10 ms).

cgi/content/full/41/2/257/DC1). Repetitive presynaptic stimulation alone (80 pulses, 1 ms duration, +150 mV, at 1 Hz) had no effect on the voltage dependence of activation of these K^+ channels (Figure 8A). However, after correlated activation at a negative interval (−6 ms), we observed a significant shift in the voltage-dependent activation curve toward more hyperpolarizing potentials (Figure 8B), suggesting that slow-inactivating K^+ channels become more readily activated during depolarization, leading to a reduction of neuronal excitability. In addition, we did not observe any significant modulation of K^+ current after correlated activation at a positive interval (Figure 8C), nor any modulation of Na^+ current at a negative interval (Figure 8D). To further test whether these slow-inactivating K^+ channels are responsible for the changes in excitability induced by correlated activity at negative intervals, we bath-applied TEA (10 mM), which is known to block most of delayed-rectifier K^+ currents (Ficker and Heinemann, 1992). As shown in Figures 8G and 8H, we found that the change in mean ISI was completely abolished, while induction of LTD was not significantly affected. Thus, the increased activation of delayed rectifier K^+ channels may account for the reduction in neuronal excitability after correlated activation that induced LTD, although we cannot exclude possible involvement of other slow-inactivating

channels that are sensitive to TEA. Finally, we note that these hippocampal cultures consist of a heterogenous population of neurons. Distinct cell types may account for the substantial variation in the profile of K^+ currents and their activation kinetics (see Figures 8A and 8E). Nevertheless, changes in the activation kinetics of slow-inactivating K^+ currents following correlated activation at negative intervals were consistently observed.

Activation of PKA is known to enhance K^+ channel activation (Schroeder et al., 1998) and thus may account for our finding that direct PKA activation by dB-cAMP can reduce neuronal firing (Figure 7H). Consistent with this idea, we observed that voltage dependence of slow-inactivating K^+ currents showed a leftward shift toward hyperpolarizing potentials following bath application of dB-cAMP (100 μM, Figure 8E). Furthermore, co-application of the PKC inhibitor Calphostin C (100 nM) together with dB-cAMP completely prevented the changes in these slow-inactivating K^+ channels (Figure 8F). These results showed that activation of PKA is sufficient to enhance the activation of these K^+ channels, hence reducing the neuronal excitability, and that the PKA effect depends on the PKC activity.

Discussion

By monitoring changes in the firing frequency of action potentials induced by a standard step depolarization, we have shown that correlated pre- and postsynaptic activation can modify the intrinsic excitability of the presynaptic neuron in a bidirectional manner that mirrors changes in synaptic efficacy, with a similar requirement for the temporal order of the pre- and postsynaptic activation (Figure 3).

The change in global neuronal excitability is not simply due to repetitive activation of the presynaptic neuron, but appears to require *trans*-synaptic retrograde signaling, the nature of which depends on the timing of pre- and postsynaptic spiking. Postsynaptic Ca^{2+} influx through NMDA receptors is required for the increase in presynaptic excitability (Ganguly et al., 2000), whereas Ca^{2+} elevation through L-type Ca^{2+} channels and Ca^{2+} released from intracellular stores are required for the reduction of presynaptic excitability (Figures 6A and 6G). Thus, it appears that different spatiotemporal patterns of Ca^{2+} elevation in the postsynaptic neuron associated with LTP and LTD can yield distinct retrograde signals, leading to increase and decrease of presynaptic excitability, respectively. Under physiological conditions, the presynaptic neuron may activate different postsynaptic cells that have distinct firing patterns, and thus may receive disparate retrograde signals that must be integrated into a coherent global change in presynaptic excitability. The molecular nature of retrograde signals associated with correlated activity is largely unknown. They may represent distinct diffusible substances that act across the synapse (Sjöström et al., 2003). Alternatively, *trans*-synaptic signaling may be conveyed by interactions between membrane bound molecules in the pre- and postsynaptic membranes in response to the correlated activity (Fitzsimonds and Poo, 1998). Our finding that the expression of LTD was unaffected by treatments with PKC and PKA inhibitors that had eliminated the reduction of presynaptic excitability (Figures 7A–7F) further suggests that the expression of LTD and the reduction of presynaptic excitability represent divergent downstream effects of postsynaptic Ca^{2+} elevation. Similar separation of the enhancement of presynaptic excitability and LTP was also observed previously (Ganguly et al., 2000). The precise postsynaptic pathways leading to these divergent effects remain to be determined.

In cortical slices, Markram et al. (1997) observed that the firing threshold and current-spiking relation in the postsynaptic neuron remain stable after the induction of LTP. In the present study, we also fail to observe any significant modification of postsynaptic excitability following correlated activation that resulted in LTP/LTD (data not shown), while marked changes in excitability were observed in presynaptic neurons. Such an asymmetric modulation of pre- and postsynaptic neuronal excitability may play an important role in the information flow within the neural network. In these hippocampal cultures, induction of LTP/LTD at glutamatergic synapses is accompanied by a rapid retrograde spread of potentiation/depression to input synapses on the dendrites of the presynaptic neuron (Fitzsimonds et al., 1997; Tao et al., 2000). In contrast, there is no forward spread of potentiation/depression to the output synapses made by the postsynaptic neuron. The rapid presynaptic spread of synaptic plasticity and global changes in the excitability may share common mechanisms, both involving cytoplasmic retrograde signals generated at the presynaptic nerve terminal as a result of correlated synaptic activity. A rapid retrograde information flow in the neural network is the basis of the back-propagation algorithm, an efficient computational procedure for supervised learning in artificial feedforward networks (Rumelhart et al., 1986; Churchland and Sejnowski, 1992). The findings of retrograde modification of presynaptic neurons support the plausibility that mechanisms resembling the back-propagation algorithm may operate in biological neural networks.

Protein kinases are known to regulate neuronal excitability through phosphorylation of voltage-gated ion channels (Madison and Nicoll, 1986; Hu et al., 1987; West et al., 1991; Schroeder et al., 1998; Hoffman and Johnston, 1998). For example, direct activation of PKC by 1-oleoyl-2-acetyl-*sn*-glycerol (OAG) can inhibit the transient Na^+ current (West et al., 1991), although OAG can also increase neuronal excitability by amplifying the persistent Na^+ current-dependent subthreshold depolarization (Franceschetti et al., 2000). In the present study, we found that treatment of cultured hippocampal neurons with PMA, a PKC activator, can also increase neuronal excitability (Figure 7G). This is consistent with the previous finding that blocking PKC activity in the presynaptic neuron inhibits the enhancement of presynaptic excitability induced by correlated activity, a process attributed to the modulation of activation and inactivation kinetics of Na^+ channels (Ganguly et al., 2000).

The PKA activity is critical for regulations of neuronal excitability and channel properties (Conn et al., 1989; Vaquero et al., 2001; Mellor et al., 2002). In the present study, we showed that activating PKA by dB-cAMP reduced presynaptic excitability (Figure 7H). Moreover, the reduction of excitability induced by correlated acti-

vation was abolished by PKA inhibitor KT 5720 (Figures 7E and 7F). That PKA activation directly underlies the reduction of excitability is further supported by the finding that PKA activation by dB-cAMP caused a leftward shift in the voltage-dependent activation curve of slow-inactivating K^+ channels (Figure 8E). Interestingly, a basal level of PKC activity is apparently necessary for the PKA's action in downregulating neuronal excitability, because PKC inhibition prevented the reduction in excitability (Figure 7H) and the modulation of K^+ channels induced by dB-cAMP (Figure 8F). This is consistent with the previous reports that showed analogous cooperation of PKC and PKA in ion channel modulation (Payet and Dupuis, 1992; Heath and Terrar, 2000).

In the previous study (Ganguly et al., 2000), the induction of LTP was found to be associated with an enhanced Na^+ channel activation, while LTD induction was found in the present study to be associated with an enhanced K^+ channel activation (Figure 8B). We did not observe any significant changes in the Na^+ channel kinetics associated with LTD induction (Figure 8D), nor have Ganguly et al. (2000) found any change in the K^+ channel kinetics following LTP induction (K. Ganguly L. Kiss, and M.-m.P., unpublished data; see also Figure 8C). Ion channels undergo dramatic modulation during development both in vivo and in vitro (McCormick and Prince, 1987; Grosse et al., 2000). In addition to correlated activation, many other kinds of electrical activity can induce the modulation of ion channels (e.g., Golowasch et al., 1999; Aizenman and Linden, 2000). Although the acute effects of correlated activation on Na^+ and K^+ channels are asymmetrical, long-term homeostatic mechanisms may maintain the overall stability and balance among various types of conductances, in an activity-dependent (reviewed in Davis and Bezprozvanny, 2001) or -independent manner (MacLean et al., 2003). Nevertheless, with regard to immediate neuronal excitability, the effects of Na^+ and K^+ channel modulation are symmetrical.

Together with the report by Ganguly et al. (2000), the findings described here have demonstrated bidirectional modification of presynaptic neuronal excitability associated with the induction of LTP and LTD. While modulation of neuronal excitability and changes in synaptic strength represent two distinct aspects of activity-induced changes in the neural circuit, they may contribute in a synergistic manner to signal processing. For example, the reliability of information transfer across the potentiated/depressed synapse may be further enhanced/reduced by a corresponding change in the reliability of presynaptic firing, resulting from changes in neuronal excitability. Furthermore, global modulation of presynaptic neuronal excitability will affect the plasticity of "upstream" synapses made onto the presynaptic neuron by modulating the initiation of back-propagating action potentials. The existence of bidirectional modification of the presynaptic excitability may thus facilitate a distributed activity-induced modification of the neural circuit, the functional consequences of which remain to be explored.

Experimental Procedures

Cell Culture Preparation and Recording

Low-density cultures of dissociated embryonic rat hippocampal neurons were prepared as described (Bi and Poo, 1998) with some modifications. Hippocampi were removed from E17 to E20 embryonic rats and treated with trypsin for 12–15 min at 37°C, followed by gentle trituration. The dissociated cells were plated at densities of 25,000 to 60,000 cells/ml on poly-L-lysine coated glass coverslips in 35 mm petri dishes. The plating medium was Dulbecco's minimum essential medium (DMEM, GIBCO) supplemented with 10% fetal calf serum (GIBCO or Hyclone, Logan, Utah), 10% Ham's F12 with glutamine (GIBCO). Twenty-four hours after plating, the culture medium was changed to the maintenance medium containing Neuro Basal Media and 5% B-27 supplement (GIBCO). This medium differs from that used in the previous study (Bi and Poo, 1998), which was 80% DMEM + 10% F-12 + 10% serum. Both glia and neurons are present under these culture conditions. Cultured neurons were used for electrophysiological recordings after 8 to 20 days in vitro.

Whole-cell perforated-patch recordings were made on two interconnected cultured hippocampal neurons. Recording pipettes were tip-filled with intracellular solution (in mM: 150 K-gluconate, 9 NaCl, 1 $MgCl_2$, 10 HEPES, 0.2 EGTA [pH 7.30]) and then back-filled with intracellular solution containing amphotericin B (150 to 220 μg/ml, Calbiochem, San Diego, CA) (Rae et al., 1991). We have carried out the experiments to test whether the patched membrane was ruptured. First, we found that ISI drifted markedly after we ruptured the membrane during whole-cell recording (see Supplemental Figure S3A at http://www.neuron.org/cgi/content/full/41/2/257/DC1). This was not the case in control experiments (Figures 2 and 4) using perforated patch configuration. Second, by loading TEA (5 mM) in the postsynaptic recording pipette, we found that in ruptured but not in perforated configuration EPSPs became significantly broadened. EPSP half-width increased from 47 ± 5 to 131 ± 13 ms (SEM, $n = 5$, $p < 0.001$, unpaired t test; Supplemental Figure S3B). The external bath solution was a HEPES-buffered (pH 7.40) saline containing (in mM): 145 NaCl, 3 KCl, 10 HEPES, 3 $CaCl_2$, 8 glucose, 2 $MgCl_2$. Throughout the experiment, the neurons were constantly perfused with fresh bath solution at a slow rate. All experiments were done at the room temperature (22°C–24°C). Recordings were done with two patch-clamp amplifiers (Axopatch 200B; Axon Inst., Foster City, CA) by methods described in Ganguly et al. (2000). For assaying synaptic connectivity, each neuron was stimulated by a 1 ms step depolarization from −70 to +80 mV in voltage-clamp mode. Only neurons with monosynaptic connections were used. We distinguish IPSCs from EPSCs by the following criteria: longer decay times, reversal potentials between −40 and −80 mV and, in some cases, sensitivity to bicuculline methiodide (10 μM, Sigma). The access resistances of both pre- and postsynaptic neurons were typically 50 MΩ. The series resistance of the postsynaptic neuron was compensated to 80% throughout the experiment. During a typical experiment, the series resistance did not change by more than 5%. The postsynaptic neuron was voltage-clamped at −70 mV, except for the assay of postsynaptic excitability, in which the neurons were current-clamped at −70 mV. The presynaptic neuron was current-clamped at −70 mV during the entire experiment, except for the experiments testing postsynaptic excitability, in which the presynaptic neurons were voltage-clamped at −70 mV. The presynaptic neuron was stimulated with current steps (0.03 to 0.2 nA, 300 to 500 ms, 0.017 Hz) to elicit a set of action potentials. Evoked EPSCs or EPSPs were recorded from the postsynaptic neuron. To determine the amount of current needed to obtain a reliable, nonsaturating presynaptic firing pattern during the control period, we tested several current intensities to estimate the current required to generate a maximal firing rate. We used the current amplitude that resulted in a firing frequency of 50% of the maximum (~4–6 spikes in 300 ms). The input resistance of the neuron was measured by injecting a step hyperpolarization (−0.05 to −0.03 nA, 200–300 ms, 0.017 Hz). Interspike intervals (ISI) were analyzed with Mini Analysis 5.0 (Synaptosoft Inc., Leonia, NJ) using a threshold level set at 50% of the spike height. The time of the peak was taken as the spike time. The ISI was measured as the interval between successive spike times. D-amino-5-phosphonopentanoic acid (D-APV, 50 μM, Sigma) and 6,7-Dinitroquinoxaline-2,3(1H, 4H) dione (DNQX, 2.0 μM, Sigma) were used to abolish glutamatergic transmission. Bicuculline (10 μM, Sigma) was used to block GABAergic transmission. To measure the change in the activation properties of the slow-inactivating K^+ channels following correlated activation, we compared populations of control neurons versus neurons that underwent correlated activation. The plateau current during the last 100 ms depolarization was

averaged for the K^+ current assessment. Slow-inactivating K^+ current was isolated by blocking Na^+ channels with tetrodotoxin (TTX, 1.0 μM), A-type channels with 2.0 mM 4-aminopyridine (4-AP, Sigma), Ca^{2+} channels and Ca^{2+}-activated K^+ channels with 100 μM $CdCl_2$ (Sigma), or nifedipine (10 μM, specific for L-type Ca^{2+} channels, Sigma) and AMPA receptor with 2.0 μM DNQX (see also Supplemental Figure S2 at http://www.neuron.org/cgi/content/full/41/2/257/DC1). Conductance densities were obtained by dividing current densities by the driving force using a calculated potassium ion equilibrium potential of −100.5 mV. Conductance-voltage (G-V) data were fitted with the Boltzmann equation ($G = G_{max}/\{1 + \exp[(V_{1/2} - V)/k]\}$) to obtain the maximal potassium conductance (G_{max}), $V_{1/2}$, and slope factor k. Na^+ currents were isolated with protocol similar to those in K^+ current, but replacing K-gluconate in the pipette solution with 55 CsCl and 75 $CsCH_3O_3$ and perfusing the bath with 100 μM $CdCl_2$ to block Ca^{2+} channels, 50 mM CsCl (Sigma), 5 mM 4-aminopyridine (Sigma), and 30 mM TEA-Cl (Sigma) to block K^+ channels; D-APV (25 μM) and DNQX (2.0 μM) to abolish glutamatergic transmission; and picrotoxin (100 μM, Sigma) to inhibit Cl^- channels. The peak amplitude of transient current was measured for Na^+ current assessment. Sodium ion equilibrium potential was calculated as +97.5 mV. Bisindolylmaleimide I hydrochloride (GF 109203X, 50 nM, Calbiochem) and Calphostin C (100 nM, Calbiochem) were used as membrane-permeable inhibitors of PKC. KT 5720 (1.0 μM, Calbiochem) was used as the membrane-permeable inhibitor of PKA. Phorbol 1,2-myristate 1,3-acetate (PMA, Calbiochem) and dibutyryl cAMP (dB-cAMP, Calbiochem) were used as the activators of PKC and PKA, respectively. We used 1,2-bis (2-aminophenoxy) ethane-N,N,N′,N′-tetraacetic acid-acetoxymethyl ester (BAPTA-AM, 2.0 mM, Molecular Probes, Eugene, OR) as a fast chelator of intracellular Ca^{2+}. For experiments with presynaptic loading of BAPTA-AM, the time of seal formation was taken as the time of onset of loading. We applied thapsigargin (1.0 μM, Calbiotech) 1 hr before correlated spiking to block Ca^{2+} released from intracellular stores.

Slice Preparation and Electrophysiology

Somatosensory cortical slices were prepared as described by Agmon and Connors (1991) and Egger et al. (1999) with some modifications. Sprague-Dawley rats (postnatal day 12–16) were anesthetized with sodium pentobarbital (50 mg/kg) and decapitated. The brain was quickly removed and immersed in ice-cold artificial cerebrospinal fluid (ACSF, composition in mM: 125 NaCl, 2.5 KCl, 1 $MgCl_2$, 2 $CaCl_2$, 1.25 NaH_2PO_4, 25 $NaHCO_3$, 25 D-glucose, bubbled with 95% O_2/5% CO_2) for 2 min. Coronal slices (300–400 μm) through the somatosensory cortex were obtained with a vibratome (Campden Instruments Ltd.) at 0°C–2°C. The slices were then incubated in ACSF at 33°C–34°C for at least 1 hr and subsequently maintained at room temperature (22°C–24°C) before recording. Pyramidal and spiny neurons in L2/3 and L4 somatosensory cortical slices were visualized and selected under infrared-differential interference contrast microscopy (Olympus, BX50WI) with a 40× water immersion objective. Patch clamping was aided by a video camera (DAGE MTI) and ScnImage software. The recording was done at 33°C–34°C. The pipette solution (300 mOsm, adjusted to pH 7.3 with KOH) contained (in mM): 105 potassium gluconate, 30 KCl, 10 HEPES, 10 phosphocreatine, 4 ATP-Mg, and 0.3 GTP. For presynaptic neurons, the pipette was tip-filled with the above solution and back-filled with the solution containing amphotericin B (150 to 220 μg/ml, Calbiochem, San Diego, CA). Typically 15 to 20 min was allowed for the perforation of presynaptic neuron, and the access resistance was about 50 Mohm. Putative postsynaptic neurons were then patched under whole-cell configuration for the detection of functional transmission. Up to six neurons are usually tested before a connected pair can be identified. The procedure for monitoring presynaptic excitability was similar to that described above for cultured neurons.

Acknowledgments

We thank J.M. Zhang, Y.R. Chen, P. Xia, and B. Wu for their help in culture preparations, X. Zhang for the help in slice experiments, and Y. Dan, K. Ganguly, H.-Z. Tao, B. Lu, X.H. Zhang, and Z.R. Wang for helpful discussions. This work was supported by grants from Major State Basic Research Program of China, the Shanghai Science and Technology Development Foundation. M.-m.P was supported in part by USNIH (NS 36999).

Received: July 2, 2003
Revised: October 20, 2003
Accepted: December 2, 2003
Published: January 21, 2004

References

Agmon, A., and Connors, B.W. (1991). Thalamocortical responses of mouse somatosensory cortex (barrel cortex) *in vitro*. Neuroscience *41*, 365–379.

Aizenman, C.D., and Linden, D.J. (2000). Rapid, synaptically driven increases in the intrinsic excitability of cerebellar deep nuclear neurons. Nat. Neurosci. *3*, 109–111.

Armano, S., Rossi, P., Taglietti, V., and D'Angelo, E. (2000). Long-term potentiation of intrinsic excitability at the mossy fiber-granule cell synapse of rat cerebellum. J. Neurosci. *20*, 5208–5216.

Bear, M.F., and Linden, D.J. (2001). The mechanisms and meaning of long-term synaptic depression in the mammalian brain. In Synapses, W.M. Cowan, T.C. Südhof, and C.F. Stevens, eds. (Baltimore, MD: Johns Hopkins University), pp. 455–517.

Beaumont, V., Zhong, N., Froemke, R.C., Ball, R.W., and Zucker, R.S. (2002). Temporal synaptic tagging by I_h activation and actin: involvement in long-term facilitation and cAMP-induced synaptic enhancement. Neuron *33*, 601–613.

Bi, G.Q., and Poo, M.M. (1998). Synaptic modifications in cultured hippocampal neurons: dependence on spike timing, synaptic strength, and postsynaptic cell type. J. Neurosci. *18*, 10464–10472.

Bliss, T.V., and Collingridge, G.L. (1993). A synaptic model of memory: long-term potentiation in the hippocampus. Nature *361*, 31–39.

Bliss, T.V., and Lømo, T. (1973). Long-lasting potentiation of synaptic transmission in the dentate area of the anaesthetized rabbit following stimulation of the perforant path. J. Physiol. *232*, 331–356.

Churchland, P.S., and Sejnowski, T.J. (1992). The Computational Brain (Cambridge, MA: MIT Press).

Conn, P.J., Strong, J.A., Azhderian, E.M., Nairn, A.C., Greengard, P., and Kaczmarek, L.K. (1989). Protein kinase inhibitors selectively block phorbol ester- or forskolin-induced changes in excitability of *Aplysia* neurons. J. Neurosci. *9*, 473–479.

Daoudal, G., Hanada, Y., and Debanne, D. (2002). Bidirectional plasticity of excitatory postsynaptic potential (EPSP)-spike coupling in CA1 hippocampal pyramidal neurons. Proc. Natl. Acad. Sci. USA *99*, 14512–14517.

Davis, G.W., and Bezprozvanny, I. (2001). Maintaining the stability of neural function: a homeostatic hypothesis. Annu. Rev. Physiol. *63*, 847–869.

Debanne, D., Gahwiler, B.H., and Thompson, S.M. (1998). Long-term synaptic plasticity between pairs of individual CA3 pyramidal cells in rat hippocampal slice cultures. J. Physiol. *507*, 237–247.

Desai, N.S., Rutherford, L.C., and Turrigiano, G.G. (1999). Plasticity in the intrinsic excitability of cortical pyramidal neurons. Nat. Neurosci. *2*, 515–520.

Egger, V., Feldmeyer, D., and Sakmann, B. (1999). Coincidence detection and changes of synaptic efficacy in spiny stellate neurons in rat barrel cortex. Nat. Neurosci. *2*, 1098–1105.

Feldman, D.E. (2000). Timing-based LTP and LTD at vertical inputs to layer II/III pyramidal cells in rat barrel cortex. Neuron *27*, 45–56.

Feldmeyer, D., Egger, V., Lübke, J., and Sakmann, B. (1999). Reliable synaptic connections between pairs of excitatory layer 4 neurons within a single 'barrel' of developing rat somatosensory cortex. J. Physiol. *521*, 169–190.

Ficker, E., and Heinemann, U. (1992). Slow and fast transient potassium currents in cultured rat hippocampal cells. J. Physiol. *445*, 431–455.

Fitzsimonds, R.M., and Poo, M.M. (1998). Retrograde signaling in the development and modification of synapses. Physiol. Rev. *78*, 143–170.

Fitzsimonds, R.M., Song, H.J., and Poo, M.M. (1997). Propagation of

activity-dependent synaptic depression in simple neural networks. Nature *388*, 439–448.

Franceschetti, S., Taverna, S., Sancini, G., Panzica, F., Lombardi, R., and Avanzini, G. (2000). Protein kinase C-dependent modulation of Na^+ currents increases the excitability of rat neocortical pyramidal neurons. J. Physiol. *528*, 291–304.

Froemke, R.C., and Dan, Y. (2002). Spike-timing-dependent synaptic modification induced by natural spike trains. Nature *416*, 433–438.

Ganguly, K., Kiss, L., and Poo, M.M. (2000). Enhancement of presynaptic neuronal excitability by correlated presynaptic and postsynaptic spiking. Nat. Neurosci. *3*, 1018–1026.

Golowasch, J., Abbott, L.F., and Marder, E. (1999). Activity-dependent regulation of potassium currents in an identified neuron of the stomatogastric ganglion of the crab *Cancer borealis*. J. Neurosci. *19*, RC33.

Grosse, G., Draguhn, A., Hohne, L., Tapp, R., Veh, R.W., and Ahnert-Hilger, G. (2000). Expression of Kv1 potassium channels in mouse hippocampal primary cultures: development and activity-dependent regulation. J. Neurosci. *20*, 1869–1882.

Heath, B.M., and Terrar, D.A. (2000). Protein kinase C enhances the rapidly activating delayed rectifier potassium current, I_{Kr}, through a reduction in C-type inactivation in guinea-pig ventricular myocytes. J. Physiol. *522*, 391–402.

Hebb, D.O. (1949). The Organization of Behavior: a Neuropsychological Theory (New York: Wiley).

Hoffman, D.A., and Johnston, D. (1998). Downregulation of transient K^+ channels in dendrites of hippocampal CA1 pyramidal neurons by activation of PKA and PKC. J. Neurosci. *18*, 3521–3528.

Hu, G.Y., Hvalby, O., Walaas, S.I., Albert, K.A., Skjeflo, P., Andersen, P., and Greengard, P. (1987). Protein kinase C injection into hippocampal pyramidal cells elicits features of long-term potentiation. Nature *328*, 426–429.

Katz, L.C., and Shatz, C.J. (1996). Synaptic activity and the construction of cortical circuits. Science *274*, 1133–1138.

Koester, H.J., and Sakmann, B. (1998). Calcium dynamics in single spines during coincident pre- and postsynaptic activity depend on relative timing of back-propagating action potentials and subthreshold excitatory postsynaptic potentials. Proc. Natl. Acad. Sci. USA *95*, 9596–9601.

Lu, U.M., Mansuy, I.M., Kandel, E.R., and Roder, J. (2000). Calcineurin-mediated LTD of GABAergic inhibition underlies the increased excitability of CA1 neurons associated with LTP. Neuron *26*, 197–205.

MacLean, J.N., Zhang, Y., Johnson, B.R., and Harris-Warrick, R.M. (2003). Activity-independent homeostasis in rhythmically active neurons. Neuron *37*, 109–120.

Madison, D.V., and Nicoll, R.A. (1986). Cyclic adenosine 3′,5′-monophosphate mediates beta-receptor actions of noradrenaline in rat hippocampal pyramidal cells. J. Physiol. *372*, 245–259.

Malenka, R.C., and Nicoll, R.A. (1999). Long-term potentiation—a decade of progress? Science *285*, 1870–1874.

Marder, E., Abbott, L.F., Turrigiano, G.G., Liu, Z., and Golowasch, J. (1996). Memory from the dynamics of intrinsic membrane currents. Proc. Natl. Acad. Sci. USA *93*, 13481–13486.

Markram, H., Lübke, J., Frotscher, M., and Sakmann, B. (1997). Regulation of synaptic efficacy by coincidence of postsynaptic APs and EPSPs. Science *275*, 213–215.

Martin, S.J., Grimwood, P.D., and Morris, R.G. (2000). Synaptic plasticity and memory: an evaluation of the hypothesis. Annu. Rev. Neurosci. *23*, 649–711.

McCormick, D.A., and Prince, D.A. (1987). Post-natal development of electrophysiological properties of rat cerebral cortical pyramidal neurons. J. Physiol. *393*, 743–762.

McCormick, D.A., Connors, B.W., Lighthall, J.W., and Prince, D.A. (1985). Comparative electrophysiology of pyramidal and sparsely spiny stellate neurons of the neocortex. J. Neurophysiol. *54*, 782–806.

McNaughton, B.L., Shen, J., Rao, G., Foster, T.C., and Barnes, C.A. (1994). Persistent increase of hippocampal presynaptic axon excitability after repetitive electrical stimulation: dependence on N-methyl-D-aspartate receptor activity, nitric-oxide synthase, and temperature. Proc. Natl. Acad. Sci. USA *91*, 4830–4834.

Mellor, J., Nicoll, R.A., and Schmitz, D. (2002). Mediation of hippocampal mossy fiber long-term potentiation by presynaptic I_h channels. Science *295*, 143–147.

Moyer, J.R., Jr., Thompson, L.T., and Disterhoft, J.F. (1996). Trace eyeblink conditioning increases CA1 excitability in a transient and learning-specific manner. J. Neurosci. *16*, 5536–5546.

Nick, T.A., and Ribera, A.B. (2000). Synaptic activity modulates presynaptic excitability. Nat. Neurosci. *3*, 142–149.

Nishiyama, M., Hong, K., Mikoshiba, K., Poo, M.M., and Kato, K. (2000). Calcium stores regulate the polarity and input specificity of synaptic modification. Nature *408*, 584–588.

Payet, M.D., and Dupuis, G. (1992). Dual regulation of the n type K^+ channel in Jurkat T lymphocytes by protein kinases A and C. J. Biol. Chem. *267*, 18270–18273.

Rae, J., Cooper, K., Gates, P., and Watsky, M. (1991). Low access resistance perforated patch recordings using amphotericin B. J. Neurosci. Methods *37*, 15–26.

Rumelhart, D.E., Hinton, G.E., and Williams, R.J. (1986). Learning internal representations by error propagation. In Parrel Distributed Processing: Explorations in the Microstructure of Cognition, volume 1, D.E. Rumelhart and J. McClelland, eds. (Cambridge, MA: MIT Press), pp. 316–362.

Schroeder, B.C., Kubisch, C., Stein, V., and Jentsch, T.J. (1998). Moderate loss of function of cyclic-AMP-modulated KCNQ2/KCNQ3 K^+ channels causes epilepsy. Nature *396*, 687–690.

Sjöström, P.J., Turrigiano, G.G., and Nelson, S.B. (2003). Neocortical LTD via coincident activation of presynaptic NMDA and cannobinoid receptors. Neuron *39*, 641–654.

Tao, H., Zhang, L.I., Bi, G.Q., and Poo, M.M. (2000). Selective presynaptic propagation of long-term potentiation in defined neural networks. J. Neurosci. *20*, 3233–3243.

Taube, J.S., and Schwartzkroin, P.A. (1988). Mechanisms of long-term potentiation: EPSP/spike dissociation, intradendritic recordings, and glutamate sensitivity. J. Neurosci. *8*, 1632–1644.

Turrigiano, G., Abbott, L.F., and Marder, E. (1994). Activity-dependent changes in the intrinsic properties of cultured neurons. Science *264*, 974–977.

Vaquero, C.F., Pignatelli, A., Partida, G.J., and Ishida, A.T. (2001). A dopamine- and protein kinase A-dependent mechanism for network adaptation in retinal ganglion cells. J. Neurosci. *21*, 8624–8635.

Wathey, J.C., Lytton, W.W., Jester, J.M., and Sejnowski, T.J. (1992). Computer simulations of EPSP-spike (E-S) potentiation in hippocampal CA1 pyramidal cells. J. Neurosci. *12*, 607–618.

West, J.W., Numann, R., Murphy, B.J., Scheuer, T., and Catterall, W.A. (1991). A phosphorylation site in the Na^+ channel required for modulation by protein kinase C. Science *254*, 866–868.

Zhang, L.I., and Poo, M.-m. (2001). Electrical activity and development of neural circuits. Nat. Neurosci. *4*, 1207–1214.

Zhang, L.I., Tao, H.W., Holt, C.E., Harris, W.A., and Poo, M.-m. (1998). A critical window for cooperation and competition among developing retinotectal synapses. Nature *395*, 37–44.